INTERNATIONAL JOURNAL OF AUTOMOTIVE SCIENCE AND TECHNOLOGY

2022, VOL. 6, NO:4, 404-411 www.ijastech.org e-ISSN: 2587-0963

The Effect of the Running Clearance to the Braking Force

Bora Güntay[1*], Aysun Baltacı[2], Cihan Kireççi[1], Özgün Cem Yılmaz[1] and Barış Oğuz Gürses[2]

Orcid Number of Author 1, Orcid Number of Author 2, Orcid Number of Author 3

[1] *Ege Fren Sanayi ve Ticaret A.Ş, İzmir, Turkey*
[2]*Department of Mechanical Engineering, Ege University, İzmir, Turkey*

Abstract

A typical air disc brake generates the braking torque by friction between rotor and pads located on both sides of the rotor. Friction causes pad and rotor to wear every time brakes are applied. As a result, a gap called running clearance is created between pads and rotor. Automatic adjuster compensates for the wear and keep the running clearance stable. If any malfunction occurs in the automatic adjuster, brake will not self-adjust and the gap will get larger.

In this study, the effect of the running clearances to the braking performance was analysed. Braking forces caused by friction between brake pads and rotor were calculated from air disc brake's mathematical model for different running clearances and compared with the experimental results.

Both the calculated and experimental results indicate that the braking force is affected from running clearance. Air chamber stroke increases proportionally as the running clearance increase but it has a physical limit. The mechanical advantage ratio of operating shaft is higher at large stroke values but it is observed that the air chamber, which provides the input force is inversely affected by the clearance after 50mm pushrod stroke. Excessive brake gap combined with high deflections caused by high input pressures overcome the operating shaft ratio increase and reduce the output force of the brake.

Keywords: air disc brake; automatic adjuster; braking force; running clearance;

Research Article
https://doi.org/10.30939/ijastech..956907

Received 24.06.2021
Revised 15.02.2022
Accepted 03.03.2022

* Corresponding author
Bora GUNTAY
bora.guntay@egefren.com.tr
Address: Ege Fren Sanayi ve Ticaret A.Ş, İzmir, Turkey University, Ankara, Turkey
Tel: +902323973653

1. Introduction

Braking systems are one of the most critical parts of vehicle dynamic system and any fault at braking system may cause serious accidents. A brake system has 3 main tasks; slowing and/or stopping a vehicle, maintaining speed when driving on a downhill and holding stationary on a downgrade. [1]

Two types of friction brakes are commonly used on heavy vehicles: drum brake and disc brake. When a drum brake is applied, linings, which are mounted on the shoes, expand and press against the inner surface of the rotating brake drum. On the other hand, a disc brake serves the same purpose by clamping the pads on both sides of the rotating brake disc. [2]

A common vehicle failure associated with braking is vehicle drifting during brake application. This issue is defined by deviation from linear path during deceleration. A light deviation can be corrected by driver steering input but an early reaction from the driver is crucial. [3]

Most modern vehicles have advances braking systems that helps brake force distribution and vehicle stability but faulty brakes are still a source of disruption for these systems. [4]

Braking forces directly affect the vehicle stability during braking and may cause vehicle pull if left and right brakes of an axle produce different braking forces. Although, the limit of the differences in braking forces on an axle is set by the authorities as 30%, vehicle manufacturers prefer to work with smaller difference values. [5]

In the previous published technical paper studied by Shridhare et al., the effect of braking force differences between left and right brakes on an axle was investigated by modelling a vehicle with the known parameters like brake force, tire properties, steering geometry, suspension hard points, vehicle CoG, scrub radius, castor angle etc. It is stated that the moment caused by the braking force difference causes the pulling problem by rotating the axle itself relative to the middle axis of the vehicle. They recommended to use tires with high lateral stiffness against this problem. [6]

Larger than normal brake running clearance may also effect the

ABS system as it limits the operating cycling frequency of brake applications. Poor brake adjustment is the source of many accidents involving trucks and a big driver of standardization of automatic brake adjustment mechanisms on air disk brakes. [7] [8]

On the other hand, smaller than normal brake running clearance has its own set of problems, such as brake drag and hot running. These problems result in more wear on brakes and rotor, increased fuel consumption and emissions. [9] [10]

The aim of this study is to calculate the braking performance efficiency for air disc brakes at different running clearances between rotor and brake pads. Braking forces which directly affect the vehicle stability during braking were calculated at different air pressure levels for different running clearances and they were compared with the experimental test results.

2. Air disc brakes

Air disc brakes have two brake pads that are clamped against the rotating disc when the brake is actuated. As the brake pads are clamped, the friction force is generated against the motion of the disc and slows the disc down.

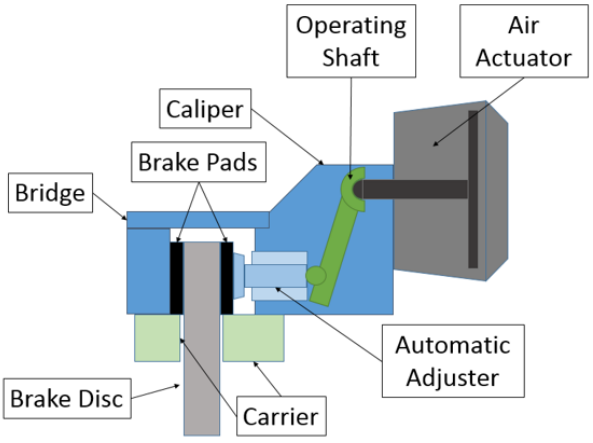

Fig. 1. Air disc brake

Air disc brake main components are illustrated in Figure 1. The air actuator is assembled to the caliper and operates the internal brake lever assembly thus removing the necessity for a conventional external lever and linkage arrangement. Sealing is provided by rubber components placed between the air actuator and housing. The carrier is mounted to the vehicle and supports the brake pads. The caliper slides on two fully sealed guide sleeves bolted to the brake carrier. As the pads wear, brake is self-adjusted by the built in automatic adjuster.

Exploded view is shown in Figure 2A. Disc brake is mounted to the axle with a brake carrier (2). There are two guide sleeves (24, 26) that are bolted on to the brake carrier by guide sleeve screws (25, 27). The caliper housing (18) is connected to and slides over the guide sleeves. The reaction force is provided on the outboard pad (3) with the help of the bridge (1) which is fixed to the caliper housing (18). Bushes (14, 16) are fixed into the housing (18) and the bridge (1) and caliper housing (18) can slide on it. The bush placed on the short guide sleeve (26) side is oval in order to accommodate brake deflection during braking. The longer sleeve (24) is round to ensure the position of the caliper housing (18). Sealing are provided externally by dust excluders (12) and end caps (28).

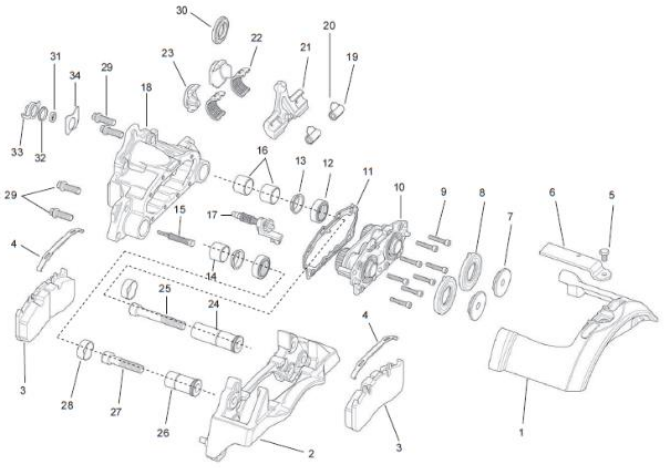

Fig. 2a. Air disc brake exploded view [11]

The operating shaft (21) amplifies the force, which is introduced from the air actuator, via its geometry. This force is transmitted to the inboard pad (3) via the half-bearings (20), the rollers (19), the tappets (36), the pistons (37) and the Piston Heads (7). When the inboard pad applies force against the rotor, the reaction force is transferred through the housing (18) and bridge (1) pulls the outboard pad towards the rotor. Braking force is created by the friction force between the brake pads and rotor. This force is transferred to the carrier at the end of the pads.

The brakes are released by reducing the clamp force of the brake. This reducing is provided by decreasing the input force on the operating shaft (21). Then the return spring (48) returns the clamping mechanism and operating shaft to their starting position and a defined running clearance between the pads and rotor is provided. The clearance between the outboard pad (3) and the rotor is generated by means of the small run out of the rotor and hub-bearing clearances.

2.1 Automatic Adjustment

The automatic adjuster adjusts the position of the brake pad to compensate for pad wear. Every time the brake is applied, the system senses whether adjustment is required or whether the running clearance of the brake pads to the brake rotor is still within the built-in tolerance and does not need to be adjusted. The built in tolerance is determined in the design by the clearance between the ball-ended drive pin (46). [11]

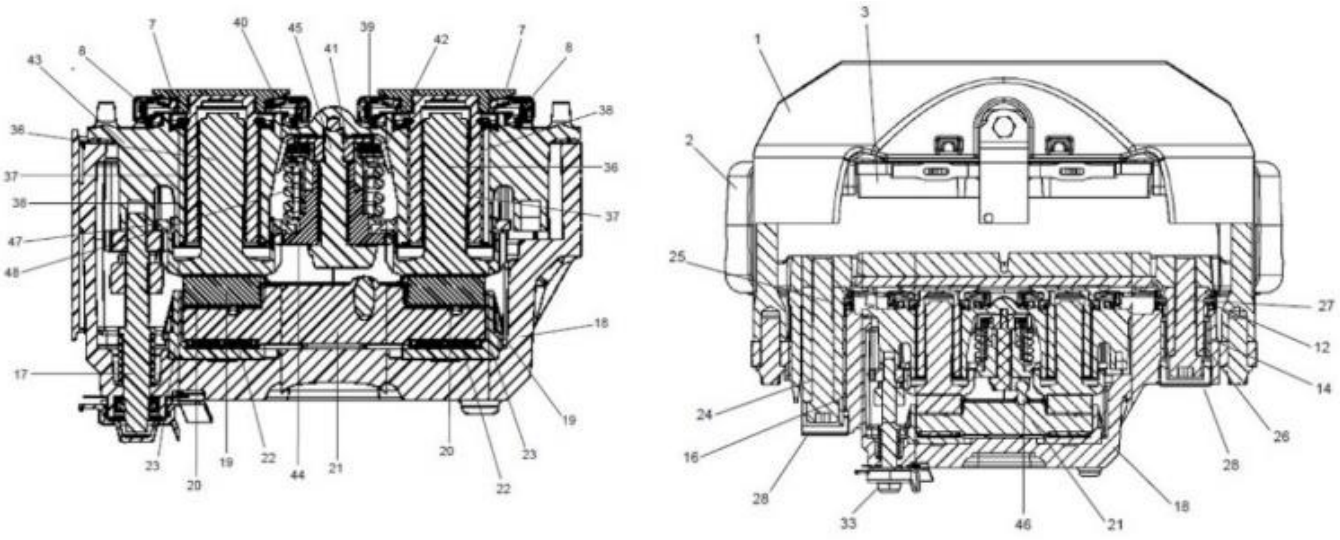

Fig. 2b. Air disc brake section view [11]

2.2 Mathematical model of air disc brake

In order to calculate the generated braking torque, air chamber and operating shaft, which transfers the push force to the rotor was modelled mathematically.

In theory, air chamber converts the incoming air pressure to pushing force directly proportioned to the surface area of the diaphragm. Air chamber push rod are shown in Figure 3.

Table 1. Air chamber mathematical equations

Symbol	Description
P	Air pressure [Bar]
A	Plate surface area [mm^2]
F_{airch}	Push force from pushrod to operating shaft [N]
S	Stroke [mm]

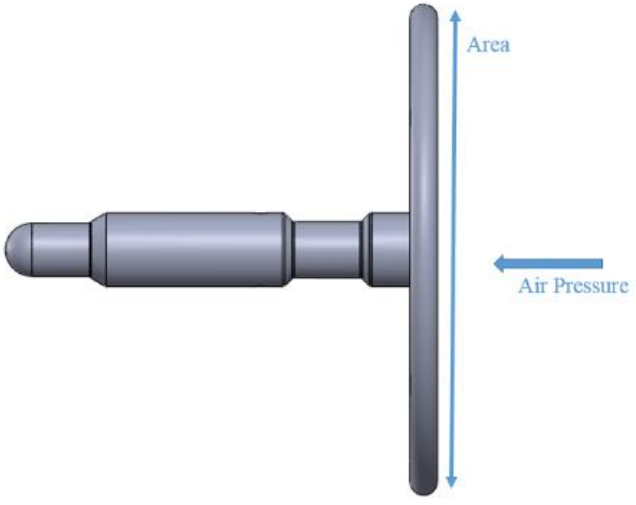

Fig. 3. Air chamber push rod

$$F_{airch}=A\times P \quad (1)$$

However, in real conditions, there are some disruptive factors such as friction and pushrod stroke distance. Due to these factors, diaphragm, which pushes the push rod by means of pressed air, bends under the influence of compressed air and cannot maintain its flatness. So linear force obtained under the pressure decreases as the diaphragm's stroke increase. An efficiency coefficient that is a function of the stroke should be added to the equation in order to compensate for this variation.

In this study, push force variation throughout full stroke of the air chamber was measured from 2 different air chambers at 3 and 6 bar air pressure in order to determine the efficiency coefficient. The results are given in Figure 4. For the most accurate representation, 6th degree least squares curve fit method with %99.52 accuracy in worst case was applied to every result obtained. Table 2 shows the results of curve fit method

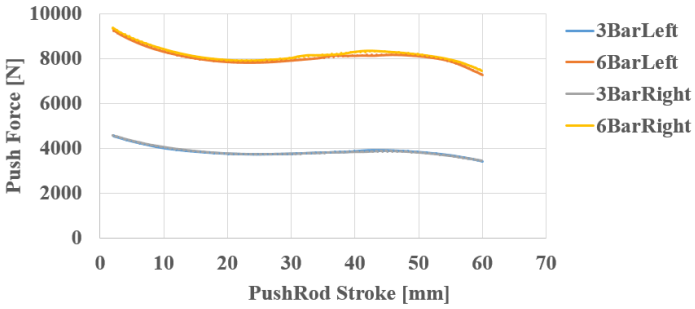

Figure 4. Push force variation due to the push rod stroke

Table 2. Curve fit polynomials

Air Pressure [Bar]	x^6	x^5	x^4	x^3	x^2	x^1	x^0
Chamber 1 at 3 bar	7.00E-07	-0.0001	0.009	-0.325	7.8132	-132.46	4812.3
Chamber 2 at 3 bar	6.00E-07	0.0001	0.0066	-0.2293	5.867	-115.78	4795.4
Chamber 1 at 6 bar	-2.00E-07	5.00E-05	-0.0056	0.1967	0.7763	-141.74	9615.9
Camber 2 at 6 bar	-8.00E-07	0.0001	-0.0089	0.2371	1.201	-149.22	9530.1
Coefficient/pressure	2.33E-07	-3.33E-05	3.00E-03	-1.08E-01	2.60E+00	-4.42E+01	1.60E+03
	2.00E-07	3.33E-05	2.20E-03	-7.64E-02	1.96E+00	-3.86E+01	1.60E+03
	-3.33E-08	8.33E-06	-9.33E-04	3.28E-02	1.29E-01	-2.36E+01	1.60E+03
	-1.33E-07	1.67E-05	-1.48E-03	3.95E-02	2.00E-01	-2.49E+01	1.59E+03
Coefficient	6.67E-08	6.25E-06	6.96E-04	-2.81E-02	1.22E+00	-3.28E+01	1.60E+03

Air chamber mathematical model was determined as the average of all curve fit polynomials.

$$F_{airch}=P(x^6S^6+x^5S^5+x^4S^4+x^3S^3+x^2S^2+x^1S^1+x^0S^0) \quad (2)$$

Push force provided by the air chamber is amplified by the mechanical ratio of the operating shaft which is nonlinear and increases with the stroke of the brake. This special nonlinear geometry is built into the operating shaft to counter the loss efficiency of the air chamber at higher strokes. In this study, stroke ratios of the input and output ends of the operating shaft was calculated by using a 3D model in order to determine the mechanical ratio. For the most accurate representation, 6th degree least squares curve fit method with %99,79 accuracy was applied to every result obtained. Operating shaft section view is shown in Figure 5 and Figure 6 illustrates the movement of operating shaft.

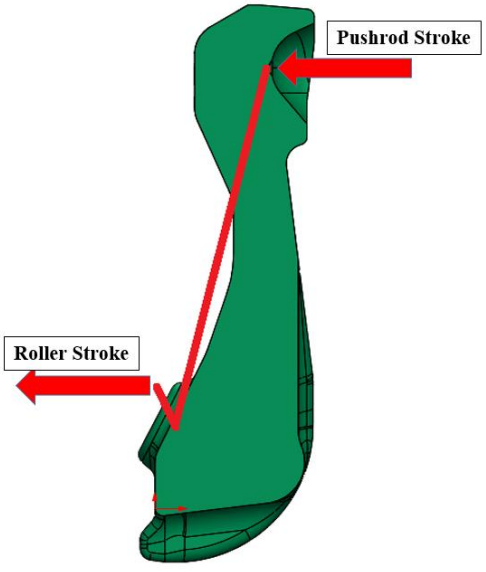

Fig. 5. Operating shaft

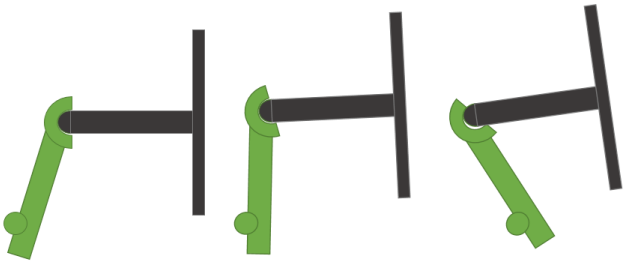

Fig. 6. Operating shaft movement

$$OpShaftMechRatio = 2.33\times10^{-10}S^6 - 3.79\times10^{-8}S^5 + 2.11\times10^{-6}S^4 - 2.14\times10^{-5}S^3 - 0.0017\times S^2 + 0.088\times S^1 + 12890 \quad (3)$$

Push force transmitted by the roller is calculated by multiplying the push force provided by the air chamber and the mechanical ratio, which is a function of the lever stroke. Where F_{roller} is push force from roller to the piston heads.

$$F_{roller}= F_{airch} \times OpshaftMechRatio \quad (4)$$

Pressured air supplied to the brake chamber creates a linear force that acts on the brake pads through brake operation shaft and rollers. Braking torque (T) is generated between the pads and the rotor. Torque generated is directly proportional to the friction (μ_B) between the pads and the rotor. As shown in Figure 7, pads actually create a distributed pressure on the rotor friction surface but this can be simplified to a force at the effective radius ($r_{effective}$)

Braking torque (T) is calculated by the equation 5.

$$T = 2 \times F_{roller} \times r_{effective} \times \mu_b \quad (5)$$

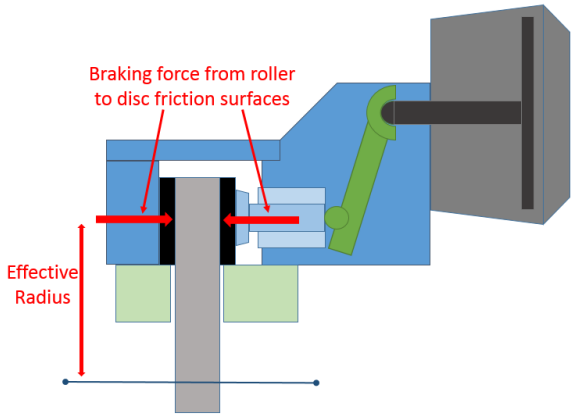

Fig. 7. Disc brake section view

3. Experimental Tests

In this study, a data acquisition system (IMC Cronosflex400) and a software (IMC Studio) was used to collect data. Stroke (Sensonics SR100W), pressure (UNIK5000), input force (custom) and output force (for 2 pistons) (Kistler 9061A) was measured. The data was collected with a sampling frequency of 1 kHz, except for the output force (because of amplifier limitations, it was collected with sampling frequency of 100 Hz).

Experiments were carried out on two identical air disc brakes with instrumented actuator.

Actuator's push rod was instrumented with a strain gauge bridge to measure brake input force. The load was calibrated through a data logger that also acts as an amplifier. [12] As seen in the Figure 8, LVDT was mounted to the back of actuator to measure brake stroke. Also a pressure sensor was used to measure input air pressure level. Output force of the brake was measured with piezoelectric load cells. The air disc brakes used for this experiment have two pistons, therefore to measure the total output force, two load cells were used.

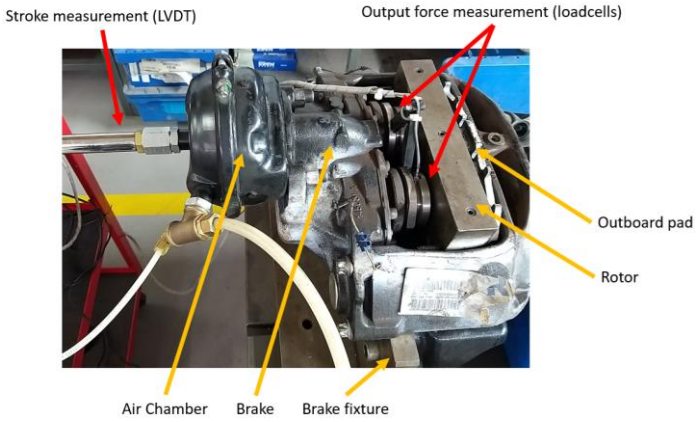

Fig. 8. Experimental setup

Experiments were carried out with air pressure level of 3 Bar (30% of max vehicle air pressure level) and 6 Bar (60% of max vehicle air pressure level). Four different pad clearances (1 mm, 1.5 mm, 2 mm, 2.5 mm) were set with a feeler gauge.

Feeler gages in general are sensitive to parallelism between the measured components. To have a more reliable initial gap, brake caliper was slid to one direction and pads were slid to opposite direction. This method concentrates two pad-rotor gaps, and two brake-pad gaps into one easier to measure volume. [13]

Brake adjuster mechanism was locked to prevent the brake from auto-adjusting. For each pad clearance, brake was applied 10 times. Input force, stroke and output force was measured at the peak pressure levels. Experimental results are given in Table 3.

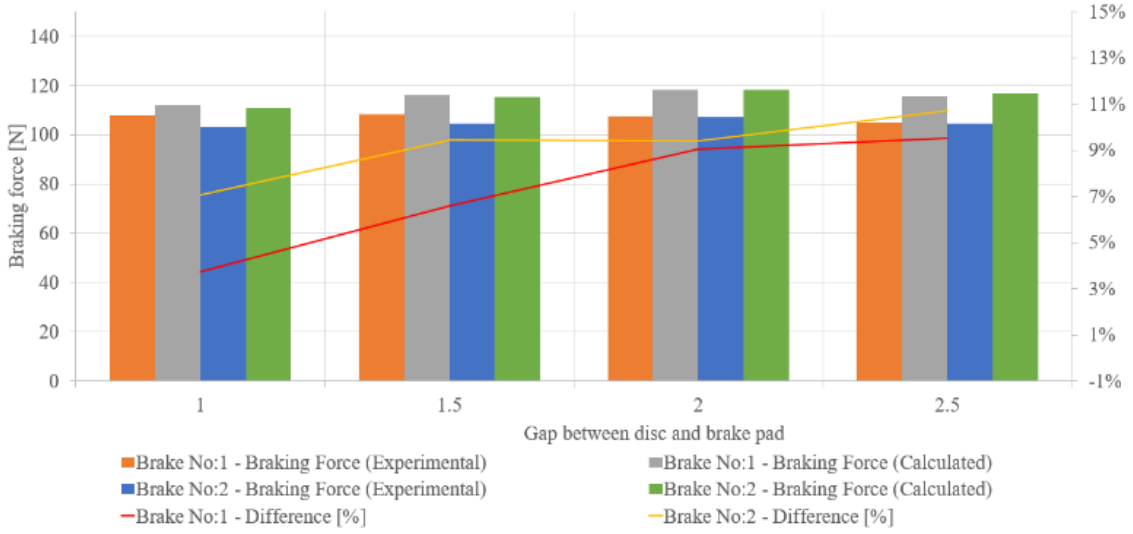

Figure 10. Comparison Bar Chart – Brake 1 and Brake 2 at 6 Bar

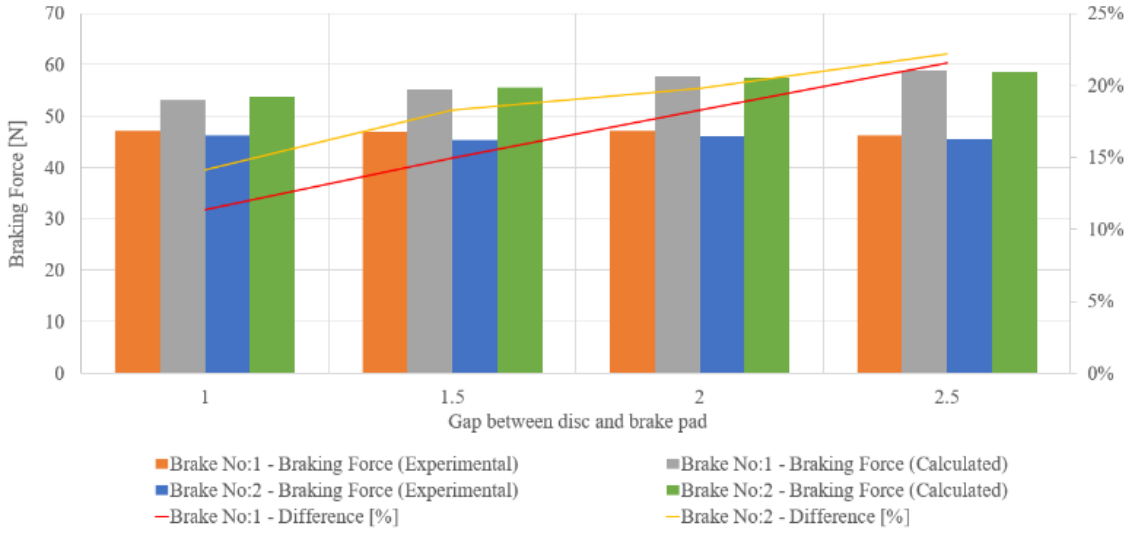

Fig. 9. Comparison Bar Chart – Brake 1 and Brake 2 at 3 Bar

Table 3. Experimental Result

Ref. Pressure	Brake number	Pad clearence	Brake Chamber Stroke	Pressure	Input force	Piston 1	Piston 2	Total output force
		[mm]	[mm]	[Bar]	[kN]	[kN]	[kN]	[kN]
3 Bar	Brake 1	1.0	27.07	2.99	3.87	27.29	19.75	47.04
		1.5	33.43	3.01	3.86	27.68	19.33	47.01
		2.0	40.07	3.02	3.98	26.88	20.20	47.08
		2.5	46.86	3.01	3.91	26.34	19.86	46.19
	Brake 2	1.0	26.36	3.04	4.24	19.76	26.42	46.18
		1.5	31.47	3.03	4.07	19.43	26.01	45.45
		2.0	39.67	3.02	4.11	19.94	26.17	46.11
		2.5	45.27	3.00	4.08	19.71	25.91	45.62
6 Bar	Brake 1	1.0	35.80	6.02	8.32	61.07	46.82	107.89
		1.5	41.60	6.03	8.32	61.58	46.66	108.24
		2.0	49.44	6.03	8.03	60.96	46.65	107.61
		2.5	56.25	6.03	7.83	59.22	45.51	104.73
	Brake 2	1.0	33.95	6.03	8.46	48.46	54.71	103.17
		1.5	40.58	6.03	8.51	48.99	55.45	104.44
		2.0	47.98	6.03	8.44	49.92	57.23	107.14
		2.5	54.71	6.03	8.12	49.04	55.30	104.34

3. Comparison of Results

In this study, test results and mathematical model was compared in various braking scenarios mentioned above. Differences between calculated and experimental braking forces in diverse air chamber strokes and running clearances at 3 Bar and 6 Bar air pressure is given in the Table 4.

At 3 Bar, air chamber stroke and the differences between calculated and experimental braking forces increase proportionally as the running clearance increases. Results at 3 Bar air pressure is given in Figure 9 and Table 5.

At 6 Bar, air chamber stroke and the differences between calculated and experimental braking forces increase as the running clearance increases. However, the increase is not linear when compared with the results at 3 Bar. Results at 6 Bar air pressure is given in the Figure 10 and Table 6.

Both the experimental results and mathematical models suggests that the output force of the brake increases with the brake running clearance until the air chamber force (input force) is inversely affected from over stroke (>50mm). This means, the brake's stopping power does start to fall off after an optimum air chamber stroke value.

Table 4. Comparison of Results

Ref. Pressure	Brake Number	Gap	Air Chamber Stroke	Air Pressure	Braking Force (Experimental)	Braking Force (Calculated)	Difference
		[mm]	[mm]	[Bar]	[kN]	[kN]	[kN]
3 Bar	Brake 1	1	27.07	2.99	47.04	53.07	11.37%
		1.5	33.43	3.01	47.01	55.25	14.92%
		2	40.07	3.02	47.08	57.61	18.28%
		2.5	46.86	3.01	46.19	58.87	21.54%
	Brake 2	1	26.36	3.04	46.18	53.78	14.13%
		1.5	31.47	3.03	45.45	55.63	18.30%
		2	39.67	3.02	46.11	57.49	19.79%
		2.5	45.27	3.00	45.62	58.61	22.16%
6 Bar	Brake 1	1	35.8	6.02	107.89	112.08	3.74%
		1.5	41.6	6.03	108.24	115.89	6.60%
		2	49.44	6.03	107.61	118.31	9.04%
		2.5	56.25	6.03	104.73	115.76	9.53%
	Brake 2	1	33.95	6.03	103.17	111.01	7.06%
		1.5	40.58	6.03	104.44	115.34	9.44%
		2	47.98	6.03	107.14	118.26	9.40%
		2.5	54.71	6.03	104.34	116.87	10.72%

Table 5. Comparison Table– Brake 1 and Brake 2 at 3 Bar

	1	1.5	2	2.5
Brake Number 1 - Braking Force (Experimental)	47.04	47.01	47.08	46.19
Brake Number 1 - Braking Force (Calculated)	53.07	55.25	57.61	58.87
Brake Number 2 - Braking Force (Experimental)	46.18	45.45	46.11	45.62
Brake Number 2 - Braking Force (Calculated)	53.78	55.63	57.46	58.61
Brake Number 1 - Difference	11.37%	14.92%	18.28%	21.54%
Brake Number 2 - Difference	14.13%	18.30%	19.79%	22.16%

Table 6. Comparison Table– Brake 1 and Brake 2 at 3 Bar

	1	1.5	2	2.5
Brake Number 1 - Braking Force (Experimental)	107.89	108.24	107.61	103.73
Brake Number 1 - Braking Force (Calculated)	112.08	115.89	118.31	115.76
Brake Number 2 - Braking Force (Experimental)	103.17	104.44	107.14	104.34
Brake Number 2 - Braking Force (Calculated)	111.01	115.34	118.26	116.87
Brake Number 1 - Difference	3.74%	6.60%	9.04%	9.53%
Brake Number 2 - Difference	7.06%	9.44%	9.40%	10.72%

4. Conclusion

The aim of the study is to demonstrate the effect of the running clearance to the braking performance at different pressure levels. In order to achieve this aim, mathematical model of the disc brake was used and it was compared with the test results.

The results show that the running clearance between the pads and rotor affects the output force of the brake. The output force increase with the brake gap as the operating shaft mechanical advantage ratio is higher at larger stroke values. But the air chamber which provides the input force is inversely affected by the clearance after 50mm pushrod stroke.

Excessive brake gap combined with high deflections caused by high input pressures overcome the operating shaft ratio increase and reduce the output force of the brake. These differences of braking force may affect the vehicle stability and may cause pulling issues at field conditions.

The study also shows that it is valuable to investigate how the brake reaction times are affected by the brake clearance.

Acknowledgment

This study was supported by Ege Fren Sanayi ve Ticaret AŞ. as researchers, we thank Ege Fren.

Conflict of Interest Statement

The authors declare that there is no conflict of interest in the study.

CRediT Author Statement

Bora Güntay: Conceptualization, methodology
Aysun Baltacı: Supervision, validation
Cihan Kireççi: Writing - original draft
Özgün Cem Yılmaz: Data curation, formal analysis
Barış Oğuz Gürses: Writing - review & editing, supervision

References

[1] Limpert, R. Brake design and safety Third Edition, SAE; 2011.
[2] Day AJ, Bryant D. Braking of road vehicles. Butterworth-Heinemann; 2022 Mar 21.
[3] Tagesson K. Truck steering system and driver interaction. Chalmers Tekniska Hogskola (Sweden); 2014.
[4] Tagesson K, Cole D. Advanced emergency braking under split friction conditions and the influence of a destabilising steering wheel torque. Vehicle system dynamics. 2017 Jul 3;55(7):970-94.
[5] Guntay B, Taşınabilir fren dinamiği inceleme cihazı tasarımı ve yazılımı [MSc Thesis]. Ege University, İzmir; 2019.
[6] Shridhare M, Sonar S, Ranawat M, Jindal AK. Estimation and Reduction of Lateral Deviation (Brake Pulling) of a Vehicle due to Difference in Left and Right Wheel Brake Force. SAE Technical Paper; 2017 Sep 17.
[7] Tretsiak D, Ivanov V. Investigation on hysteresis losses into disc brake gear for heavy vehicles. SAE paper. 2006 Oct 8:01-3212.
[8] Henock A. Design Improvement On The Brake Clearance Adjustment Of Sino-Truck (Doctoral dissertation).
[9] Tamasho T, Doi K, Hamabe T, Koshimizu N, Suzuki S. Technique for reducing brake drag torque in the non-braking mode. JSAE review. 2000 Jan 1;21(1):67-72.
[10] Antaaitis DB. Vehicle Level Brake Drag Target Setting for EPA Fuel Economy Certification. SAE International Journal of Passenger Cars-Mechanical Systems. 2016 Sep 18;9(2016-01-1925):1157-71.
[11] Maintenance Manual no. MM-0350 ELSA 195/225 Reaction Beam Air Disc Brake; 2009.
[12] Corminboeuf D. Calibration of bridge standard for strain gauge bridge amplifier. In17th International Congress of Metrology 2015 (p. 04004). EDP Sciences.
[13] D'Emilia G, Gaspari A, Iavicoli C, Natale E. Measurement uncertainty estimation of gap and profile in the automotive sector. InJournal of Physics: Conference Series 2020 Jul 1 (Vol. 1589, No. 1, p. 012017). IOP Publishing.